Synthesis and properties of Fe^{III} and Co^{III} complexes: structures of [(L^2)Fe(N$_3$)$_3$], [(L^2)$_2$Fe$_2$(μ-O)(μ-O$_2$CMe)$_2$][ClO$_4$]$_2$·2H$_2$O and [(L^2)$_2$Co$_2$(μ-OH)$_2$(μ-O$_2$CMe)][ClO$_4$]$_3$·MeCN [L^2 = methyl[2-(2-pyridyl)ethyl](2-pyridylmethyl)amine] †

Jhumpa Mukherjee, V. Balamurugan, Rajeev Gupta and Rabindranath Mukherjee *

*Department of Chemistry, Indian Institute of Technology, Kanpur 208 016, India.
E-mail: rnm@iitk.ac.in; Fax: +91-512-2597437*

Three mononuclear half-sandwich iron(III) ($S = \frac{1}{2}$) complexes [(L^2/L^3)FeCl$_3$]·H$_2$O (1/2) and [(L^2)Fe(N$_3$)$_3$] (3) have been synthesized and their properties investigated [L^2 = methyl[2-(2-pyridyl)ethyl](2-pyridylmethyl)amine; L^3 = *N*-methyl-*N*,*N*-bis(2-pyridylmethyl)amine]. X-ray structural analysis revealed that in 3 the FeN$_6$ unit is attained by co-ordination of three nitrogens of facially capping L^2 and three azide nitrogens. The X-ray structural results on [(L^2)$_2$Fe$_2$(μ-O)(μ-O$_2$CMe)$_2$][ClO$_4$]$_2$·2H$_2$O (4), revealed a bioctahedral structure with one oxo and two bridging acetate ligands, similar to that found in various forms of marine invertebrate oxygen transport protein, haemerythrin. Temperature-dependent (51–300 K) magnetic susceptibility measurements revealed for complex 4, $J = -130$ cm^{-1}, and for a brownish orange diiron(III) complex [(L^3)$_2$Fe$_2$(μ-O)(μ-O$_2$CMe)$_2$][ClO$_4$]$_2$·2H$_2$O (5), $J = -114$ cm^{-1}, demonstrating that the extent of exchange coupling is more for the complex with unsymmetrical terminal ligand L^2 than that with symmetrical ligand L^3. A new binuclear triply-bridged dicobalt(III) complex [(L^2)$_2$Co$_2$(μ-OH)$_2$-(μ-O$_2$CMe)][ClO$_4$]$_3$·MeCN (6) has been synthesized, structurally characterized (L^2 is terminally co-ordinated in a facial mode) and its spectroscopic and redox properties investigated. To the best of our knowledge, this is the first structural report for a such a core formation with a facially capping tridentate N-donor ligand. The redox behaviour of mononuclear and dinuclear complexes has been investigated by cyclic voltammetry, and the results rationalized.

Introduction

The (μ-oxo)bis(μ-carboxylato)diiron(III) core is well established in the structure of haemerythrin, a marine invertebrate respiratory protein, in its various forms.[1] The past twenty years have witnessed an upsurge of interest in the syntheses of complexes having such cores, utilizing a variety of facially capping tridentate nitrogen donor ligands. Detailed overviews of characterized diferric model complexes can be found in the literature.[2] To search for a synthetic model of met-azidohemerythrin the synthesis, spectroscopic and temperature-dependent magnetic and chemical reactivity properties (bridge-exchange reactions) of diiron(III) complexes containing the triply bridged Fe$_2$(μ-O)(μ-X)$_2$ core (X = MeCO$_2$, PhCO$_2$ or (PhO)$_2$PO$_2$] were achieved by using terminally an unsymmetrical tridentate ligand L^1 and its N-methylated derivative L^2.[3]

The iron complexes "LFe^{III}X$_3$" [L = 1,4,7-triazacyclononane (TACN), 1,4,7-trimethyl-1,4,7-triazacyclononane (Me$_3$TACN), hydrotris(1-pyrazolyl)borate HB(pz)$_3^-$ or hydrotris(3,5-dimethyl-1-pyrazolyl)borate HB(3,5-Me$_2$pz)$_3^-$); X = Cl$^-$ or N$_3^-$ or CN$^-$][4] were reported to be good reactants for syntheses of a series of interesting iron complexes. From this viewpoint we synthesized [(L^2)FeCl$_3$]·H$_2$O (1). To investigate (i) the effect of five-membered/six-membered chelate ring on the properties of such complexes and (ii) the substitutional flexibility of Cl$^-$ ions present in 1, we have prepared the complexes [(L^3)FeCl$_3$]·H$_2$O (2) and [(L^2)Fe(N$_3$)$_3$] (3), and structurally characterized 3. The structure of [(L^2)$_2$Fe$_2$(μ-O)(μ-O$_2$CMe)$_2$][ClO$_4$]$_2$·2H$_2$O (4) was determined to authenticate our previous claim[3] of formation of a (μ-oxo)bis(μ-carboxylato)diiron(III) core. To pinpoint, if any, the effect of the five-membered/six-membered chelate ring on the magnetic and redox properties of such a core an orange–brown complex [(L^3)$_2$Fe$_2$(μ-O)(μ-O$_2$CMe)$_2$][ClO$_4$]$_2$·

2H$_2$O (5) (a green complex [(L^3)$_2$Fe$_2$(μ-O)(μ-O$_2$CMe)$_2$][ClO$_4$]$_2$·2H$_2$O was structurally characterized)[5] has been synthesized, utilizing [Fe$_2$OCl$_6$]$^{2-}$ as the starting material. As a part of our bio-inspired syntheses of [(L^2)$_2$Mn^{III}$_2$(μ-O)(μ-O$_2$CMe)$_2$]$^{2+}$, [(L^2)$_2$Mn^{III}Mn^{IV}(μ-O)$_2$(μ-O$_2$CMe)]$^{2+}$ and [(L^2)$_2$Mn^{IV}$_2$(μ-O)$_2$-(μ-O$_2$CMe)]$^{3+}$ cores,[6,7] and also of [(L^2)$_2$Ru^{III}$_2$(μ-O)(μ-O$_2$-CMe)$_2$]$^{2+}$ [8] with use of the tridentate facially capping ligand with chelate ring asymmetry (L^2) we directed our attention towards a dimeric cobalt(III) complex. Moreover, we have now extended the formation of a triply-bridged core to cobalt(III), [Co$_2$(μ-OH)$_2$(μ-O$_2$CMe)(L)$_2$][ClO$_4$]$_3$·MeCN (6), structurally chacterized it and studied its properties. Here we report the outcome of such an investigation.

Experimental

Reagents and materials

All chemicals were obtained from commercial sources and used as received. Solvents were dried as reported previously.[3,6–8] [Et$_4$N]$_2$[Fe$_2$OCl$_6$][9] and [n-Bu$_4$N][ClO$_4$][8] were prepared as before.

R = H; L^1
R = Me; L^2 L^3
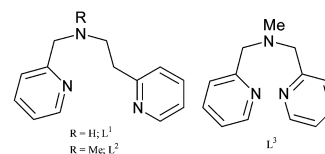
Syntheses

N-Methyl-*N*,*N*-bis(2-pyridylmethyl)amine, L^3. The methodology followed here to prepare this ligand is different from that already reported.[5] 2-Picolyl chloride hydrochloride (2 g, 12.2 mmol) was taken in ethanol (5 cm^3) and placed over an ice-bath. To it was added a saturated aqueous solution of K$_2$CO$_3$, under vigorous magnetic stirring, up to complete neutralization (pH ~ 7). The mixture was then filtered (solution A). Separately,

† Electronic supplementary information (ESI) available: Fig. S1–S3 discussed in the text. See http://www.rsc.org/suppdata/dt/b3/b305470e/

a mixture of a 40% aqueous solution of MeNH$_2$ and Et$_3$N (1.23 g, 12.2 mmol) was taken in ethylacetate (10 cm^3) (solution B). Solution A was added dropwise to solution B. The resulting mixture was stirred for 5 days at 300 K. After filtration, the solvent was removed under reduced pressure to give a dark yellow oil, from which the desired product was repeatedly extracted using ethylacetate (3 × 5 cm^3). The combined organic layer was dried over anhydrous Na$_2$SO$_4$. Solvent removal afforded a yellow oil (yield: 1.0 g, 77%). ^{1}H NMR (CDCl$_3$, 80 MHz): δ 8.4 (2H, d, pyridine 6-H), 7.7–6.9 (6H, m, pyridine 3,4,5-H), 3.7 (4H, s, NCH$_2$), 2.2 (3H, s, NMe).

Syntheses of the complexes

[(L^2)FeCl$_3$]·H$_2$O (1). To a solution of anhydrous FeCl$_3$ (0.036 g, 0.220 mmol) in EtOH (2 cm^3) was added a solution of L^2 (0.050 g, 0.220 mmol) in EtOH (1 cm^3). The solution was stirred for 15 min and the orange microcrystalline precipitate that formed was collected by filtration, washed with EtOH:Et$_2$O (1:4 v/v) mixture (5 cm^3) and dried *in vacuo* (yield: 0.055 g, ~60%). Found: C, 41.00; H, 4.25; N, 10.33. Calc for C$_{14}$H$_{19}$Cl$_3$FeN$_3$O: C, 41.24; H, 4.66; N, 10.31%. IR (KBr disc, selected peaks): 3420 cm^{-1} (ν(OH) of water of crystallisation). Molar conductance, Λ_M (MeCN, ≈1 mol dm^{-3} solution at 298 K) = 60 Ω^{-1} cm^2 mol^{-1} (expected range [10] for 1:1 electrolyte: 120–160 Ω^{-1} cm^2 mol^{-1}). Absorption spectrum [λ_{max}, nm (ε, dm^3 mol^{-1} cm^{-1})]: (in MeCN) 245 (11 600), 309 (6600), 356 (4900).

[(L^3)FeCl$_3$]·H$_2$O (2). To a solution of anhydrous FeCl$_3$ (0.036 g, 0.220 mmol) in EtOH (2 cm^3) was added a solution of L^3 (0.050 g, 0.220 mmol) in EtOH (1 cm^3). The solution was stirred for 15 min and the orange microcrystalline precipitate that formed was collected by filtration, was washed with EtOH:Et$_2$O (1:4 v/v) mixture (5 cm^3) and dried *in vacuo* (yield: 0.055 g, ~60%). Found: C, 39.65; H, 4.36; N, 10.56. Calc for C$_{13}$H$_{17}$Cl$_3$FeN$_3$O: C, 39.66; H, 4.32; N, 10.68%. IR (KBr disc, selected peaks): 3440 cm^{-1} (ν(OH) of water of crystallisation). Molar conductance, Λ_M (MeCN, ≈1 mol dm^{-3} solution at 298 K) = 50 Ω^{-1} cm^2 mol^{-1}. Absorption spectrum [λ_{max}, nm (ε, dm^3 mol^{-1} cm^{-1})]: (in MeCN) 252 (7200), 304 sh (3820), 372 (2460).

[(L^2)Fe(N$_3$)$_3$] (3). To an orange–yellow suspension of [(L^2)FeCl$_3$]·H$_2$O (0.050 g, 0.123 mmol) in MeCN (5 mL) was added solid NaN$_3$ (0.032 g, 0.492 mmol). The resulting deep red solution was stirred for 30 min and filtered. Slow evaporation of the filtrate resulted in the formation of red coloured crystals which were collected by filtration, washed with MeCN:Et$_2$O (1:4 v/v) mixture (5 cm^3). Finally the compound was dried *in vacuo* (yield: 0.034 g, ~ 68%). Found: C, 40.93; H, 4.24; N, 41.72. Calcd for C$_{14}$H$_{17}$N$_{12}$Fe: C, 41.09; H, 4.16; N, 41.09%. IR (KBr disc, selected peaks): 2090 cm^{-1} (ν(N$_3^-$)). Molar conductance, Λ_M (MeCN, ≈1 mol dm^{-3} solution at 298 K) = 50 Ω^{-1} cm^2 mol^{-1}. Absorption spectrum [λ_{max}, nm (ε, dm^3 mol^{-1} cm^{-1})]: (in MeCN) 252 (18 000), 332 (6900), 506 (5000).

[(L)$_2$Fe$_2$(μ-O)(μ-O$_2$CMe)$_2$][ClO$_4$]$_2$·2H$_2$O (4). The complex was prepared following a previously reported procedure.[3] Single crystals suitable for X-ray crystallographic studies were grown by vapour diffusion of ethylacetate to a MeCN solution of the complex.

[(L^3)$_2$Fe$_2$(μ-O)(μ-O$_2$CMe)$_2$][ClO$_4$]$_2$·2H$_2$O (5). A mixture of [Et$_4$N]$_2$[Fe$_2$OCl$_6$] (0.100 g, 0.166 mmol) and NaO$_2$CMe (0.028 g, 0.332 mmol) in MeCN (5 cm^3) was stirred for 20 min. The ligand L^3 (0.071 g, 0.332 mmol) dissolved in MeCN (5 cm^3) was added dropwise to it over a period of 10 min. The above mixture was stirred at room temperature for 4 h. Solid NaClO$_4$·H$_2$O (0.074 g, 0.526 mmol) was added to it and stirred for another 15 min, filtered and solvent was removed under reduced pressure at 30–40 °C. The solid obtained was dissolved in

MeCN (5 cm^3), filtered and kept for slow evaporation. Brown crystals that formed was collected by filtration and washed with MeCN:EtOAc (1:4; v/v) mixture (5 cm^3). Recrystallisation was achieved by diffusion of EtOAc into a MeCN solution (yield: 0.100 g, ~67%). Found: C, 39.82; H, 4.53; N, 9.70. Calcd for C$_{30}$H$_{40}$N$_6$O$_{15}$Cl$_2$Fe$_2$: C, 39.70; H, 4.41; N, 9.26%. IR (KBr disc, selected peaks): 3431 (ν(OH)), 1558 and 1300 (ν(O$_2$CMe)), 1091 and 624 (ν(ClO$_4^-$)) cm^{-1}. Molar conductance, Λ_M (MeCN, ≈1 mol dm^{-3} solution at 298 K) = 220 Ω^{-1} cm^2 mol^{-1} (expected range [10] for 1:2 electrolyte: 220–300 Ω^{-1} cm^2 mol^{-1}). Absorption spectrum [λ_{max}, nm (ε, dm^3 mol^{-1} cm^{-1})]: (in MeCN) 235 (23 800), 340 (7300), 380 (4400), 420 sh (1400), 458 (1300), 503 (990), 540 sh (250), 702 (280).

[(L^2)$_2$Co$_2$(μ-OH)$_2$(μ-O$_2$CMe)][ClO$_4$]$_3$·MeCN (6). To a solution of L^2 (0.100 g, 0.447 mmol) in MeOH (5 cm^3), a solution of Co(O$_2$CMe)$_2$·4H$_2$O (0.100 g, 0.441 mmol) in MeOH (5 cm^3) was added dropwise, under magnetic stirring. The resulting reddish brown solution was stirred for 30 min and to it solid NaClO$_4$·H$_2$O (0.200 g, 1.42 mmol) was added. It was stirred for a further 2 h and the resulting solution was then concentrated to half of its original volume. Slow evaporation of the above solution resulted in the formation of red coloured crystals within a day. The compound was collected by filtration and washed with cold MeOH (5 cm^3) (yield: 0.115 g, ~52%). Found: C, 38.16; H, 4.19; N, 10.02. Calcd for C$_{32}$H$_{42}$N$_7$O$_{16}$Cl$_3$Co$_2$: C, 38.23; H, 4.18; N, 9.76%. IR (KBr disc, selected peaks): 3413 (ν(OH)), 1543 and 1447 (ν(O$_2$CMe)), 1081 and 626 (ν(ClO$_4^-$)) cm^{-1}. Molar conductance, Λ_M (MeCN, ≈1 mol dm^{-3} solution at 298 K) = 343 Ω^{-1} cm^2 mol^{-1} (expected range [10] for 1:3 electrolyte: 340–420 Ω^{-1} cm^2 mol^{-1}). Absorption spectrum [λ_{max}, nm (ε,. dm^3 mol^{-1} cm^{-1})]: (in MeCN) 253 sh (33 400), 330 (5500), 540 (220).

CAUTION: perchlorate salts of compounds containing organic ligands are potentially explosive!

Physical measurements

Elemental analyses (C, H, N) were obtained at the Micro-analysis Service Centre at this Department. Infrared spectra were recorded on a Brüker Vector 22 spectrophotometer using KBr discs. Electronic spectra were recorded either using a Perkin Elmer Lambda 2 or Agilent 8453 diode-array spectrophotometer. Solution electrical conductivity measurements (25 °C) were carried out with an Elico (Hyderabad, India) Type CM-82 T conductivity bridge.

Magnetism

Variable temperature (81–300 K for **1**–**3** and 51–300 K for **4** and **5**) magnetic susceptibilities measurements in the solid state were performed using a locally-built Faraday balance [11] comprising an electromagnet with constant gradient pole caps (Polytronic Corporation, Mumbai, India), an ultravacuum Sartorius M25-D/S Balance (Germany), a closed-cycle refrigerator and a Lake Shore temperature controller (Cryo Industries, USA). All measurements were made at a fixed main field strength of ~ 6 kG. Solution state magnetic susceptibility was obtained by the NMR technique of Evans [12] in MeCN with a PMX-60 JEOL (60 MHz) NMR spectrometer. Susceptibilities were corrected for the diamagnetic contribution, by using literature values.[13] Effective magnetic moments were calculated from $\mu_{eff} = 2.828 [\chi_M T]^{1/2}$, where χ_M is the corrected molar susceptibility.

Cyclic voltammetry

Cyclic voltammograms were recorded at 298 K on PAR model 370 electrochemistry system consisting of a model 174A polarographic analyzer and a model 175 universal programmer. A standard three-electrode cell was employed with either a PAR model G0021 glassy carbon working electrode or a Beckman

Table 1 Data collection and structure refinement parameters for $[(L^2)Fe(N_3)_3]$ (**3**), $[(L^2)_2Fe_2(\mu\text{-O})(\mu\text{-O}_2CMe)_2][ClO_4]_2\cdot2H_2O$ (**4**) and $[(L^2)_2Co_2$-$(\mu\text{-OH})_2(\mu\text{-O}_2CMe)][ClO_4]_3\cdot MeCN$ (**6**)

Complex	3	4	6
Molecular formula	$C_{14}H_{17}FeN_{12}$	$C_{32}H_{44}Cl_2N_6O_{15}Fe_2$	$C_{32}H_{42}Cl_3N_7O_{16}Co_2$
M_r	409.25	935.33	1004.94
Temperature/K	293(2)	293(2)	150(2)
Radiation used ($\lambda/\text{Å}$)	Mo Kα (0.71073)	Mo Kα (0.71073)	Mo Kα (0.71073)
Crystal system	Orthorhombic	Orthorhombic	Orthorhombic
Space group	$Pc2_1n$ (no. 33)	$P2_1nb$ (no. 33)	$P2_12_12_1$ (no. 19)
$a/\text{Å}$	8.526(5)	13.453(6)	12.699(2)
$b/\text{Å}$	14.119(5)	17.69(2)	17.571(3)
$c/\text{Å}$	15.250(5)	18.692(8)	18.091(3)
$V/\text{Å}^3$	1835.8(14)	4449(7)	4036.8(12)
Z	4	4	4
D_c/g cm^{-3}	1.481	1.396	1.654
μ/mm^{-1}	0.849	0.839	1.100
Crystal size/mm	$0.40 \times 0.30 \times 0.40$	$0.30 \times 0.20 \times 0.20$	$0.30 \times 0.20 \times 0.20$
Unique reflections, R_{int}	1687, 0.0000	2969, 0.2699	9575, 0.0642
Observed reflections ($I > 2\sigma(I)$)	1130	1237	6479
Refined parameters	244	216	542
$R(F, F^2 > 2\sigma)$ (R_w)	0.0546 (0.1278)	0.1010 (0.2328)	0.0494 (0.1036)
$R(F$, all data) (R_w)	0.0972 (0.1483)	0.2369 (0.3235)	0.0830 (0.1165)
Absolute structure factor	0.05(8)	$-0.04(16)$	0.509(19)
Goodness-of-fit on F^2	1.008	1.004	0.947
Max./min. electron density/e Å^{-3}	0.390, -0.461	0.845, -0.665	0.722, -0.616

platinum inlay electrode (M 39273), a platinum-wire auxiliary electrode and a saturated calomel electrode (SCE) as reference; no corrections were made for junction potentials. Details of cell configuration and criterion for reversibility are as reported previously.[8]

Crystallography

The data on complex **3** were collected at room temperature on a Siemens P4 diffractometer, with graphite-monochromated Mo Kα radiation (λ = 0.71073 Å). The data were corrected for Lorentz and polarization factors. The structure was solved by direct methods (SIR-92) and refined (SHELXL 97) by full matrix least squares methods based on F^2. These programs were accessed through WINGX 1.64 crystallographic collective package.[14] All non-hydrogen atoms were refined anisotropically. Hydrogen atoms were fixed geometrically and were not refined.

Crystal data on complex **4** were collected on a Enraf Nonius MACH2 diffractometer and on a BRUKER SMART diffractometer/CCD area detector for complex **6**, equipped with graphite-monochromated Mo Kα radiation (λ = 0.71073 Å). Data were corrected for Lorentz and polarization effects. The structures were solved with SIR-92 and refined with the SHELXL-97 package incorporated in WINGX 1.64 crystallographic collective package.[14] Anisotropic refinements were performed by full-matrix least-squares procedure on F^2. The positions of the hydrogen atoms were calculated assuming ideal geometries, but not refined. For **6**, all atoms were refined anisotropically. For **4**, except a few C atoms (acetate carbons, methyl and methylene C atoms), N-methyl N atoms, which were refined isotropically, all other atoms were refined with anisotropic thermal parameters. Quite a few bonds were restrained to get reasonable distances and all four pyridyl rings were anisotropically refined, as a group. We could not locate the hydrogen atoms of the water molecules. Quite a few reflections (26) were omitted in the final stages of refinement, as the peak profiles were extremely broad. These erroneous reflections were probably caused by the quality of crystal chosen for data collection. The quality of crystal obtained was not at all good (high R_{int} values), which could be the reason for higher R values observed. Unfortunately, we could not grow single crystals of **4** that were any better than the one used for the present study, as they were the best we could have. The overall structure refinement was poor and hence the crystallographic results will not be reported in detail. Crystal data, data collection, and refinement parameters **3**, **4** and **6** are listed in Table 1.

CCDC reference numbers 209228 (**3**), 208229 (**4**) and 209230 (**6**).

See http://www.rsc.org/suppdata/dt/b3/b305470e/ for crystallographic data in CIF or other electronic format.

Results and discussion

Syntheses

We found that mononuclear half-sandwich iron(III) complexes $[(L^2/L^3)FeCl_3]\cdot H_2O$ (**1/2**) can readily be synthesized from the reaction between anhydrous $FeCl_3$ and L^2/L^3 in EtOH. Controlled reaction of **1** with NaN_3 afforded isolation of $[(L^2)Fe(N_3)_3]$ (**3**). The structure of **3** was unequivocally determined by X-ray crystallography (*vide infra*).

Although synthesis and structural characterization of a green complex $[(L^3)_2Fe_2(\mu\text{-O})(\mu\text{-O}_2CMe)_2][ClO_4]_2\cdot2H_2O$ was reported in the literature,[5] we followed a synthetic procedure starting from a preformed (oxo-bridged)diiron(III) species $[Fe_2OCl_6]^{2-}$ as the source of iron(III), to isolate an orange–brown solid (**5**) of identical composition. Unfortunately, the single crystals obtained for **5** turned out to be twinned. However, dissolution of the orange–brown crystals into MeCN gives identical spectra (*vide infra*) as reported by McKenzie and coworkers[5] and temperature-dependent magnetic studies (*vide infra*) give identical behaviour. It appears that it is the differences in the unit cell packing (which the presence of solvent molecules in different form could induce) that are responsible for the variations in the observed solid-state colour. Interestingly, two different coloured single crystals, one with and the other without solvent of crystallization, of a similar core (however, dimer-of-dimer type) with strapped TACN were obtained and their structures determined.[15]

Reaction between $Co(O_2CMe)_2\cdot4H_2O$, L^2 and $NaClO_4\cdot H_2O$ in MeOH afforded isolation of a new complex $[(L^2)_2Co_2$-$(\mu\text{-OH})_2(\mu\text{-O}_2CMe)][ClO_4]_3\cdot MeCN$ (**6**), after recrystallisation from MeCN/Et$_2$O.

As expected, compounds **1**, **2** and **3** are non-electrolyte in MeCN solution. The orange–brown complex **5** exhibited the IR bands corresponding to bridging acetate, FeOFe moiety, water of crystallisation and ClO_4^-. The red crystals of complex **6** exhibited the characteristic IR bands assignable to bridging acetate, $\nu(OH)$ and ClO_4^-. In MeCN solution, the compound **6** behaves as a 1:3 electrolyte. Elemental analyses, IR and solution electrical conductivity data are in agreement with the above formulations for all new complexes.

Table 2 Selected bond lengths (Å) and angles (°) of $[(L^2)Fe(N_3)_3]$, (**3**) and $[(L^2)_2Co_2(\mu\text{-}OH)_2(\mu\text{-}O_2CMe)][ClO_4]_3\cdot MeCN$, (**6**)

| **3**		**6**	
Fe–N(1)	2.214(14)	Co(1)–O(1)	1.917(3)
Fe–N(2)	2.246(8)	Co(1)–O(2)	1.911(3)
Fe–N(3)	2.204(13)	Co(1)–O(3)	1.884(3)
Fe–N(4)	1.977(7)	Co(1)–N(1)	1.969(4)
Fe–N(7)	1.978(17)	Co(1)–N(2)	2.000(4)
Fe–N(10)	2.040(13)	Co(1)–N(3)	1.935(4)
N(4)–N(5)	1.168(9)	Co(2)–O(1)	1.914(3)
N(5)–N(6)	1.124(11)	Co(2)–O(2)	1.917(3)
N(7)–N(8)	1.10(2)	Co(2)–O(4)	1.896(3)
N(8)–N(9)	1.21(2)	Co(2)–N(4)	1.924(4)
N(10)–N(11)	1.160(18)	Co(2)–N(5)	2.010(4)
N(11)–N(12)	1.068(18)	Co(2)–N(6)	1.970(4)
N(3)–Fe–N(4)	91.0(6)	Co(1)–Co(2)	2.8781(9)
N(1)–Fe–N(2)	87.5(4)	Co(1)–O(1)–Co(2)	97.39(12)
N(1)–Fe–N(3)	85.01(19)	Co(1)–O(2)–Co(2)	97.52(12)
N(2)–Fe–N(3)	77.0(4)	N(1)–Co(1)–O(1)	93.08(14)
N(3)–Fe–N(7)	89.9(6)	N(1)–Co(1)–O(2)	172.27(14)
N(3)–Fe–N(10)	169.5(6)	N(2)–Co(1)–O(1)	172.10(14)
N(4)–N(5)–N(6)	173(3)	N(2)–Co(1)–O(3)	89.44(15)
N(7)–N(8)–N(9)	165(3)	N(3)–Co(1)–O(1)	93.54(14)
N(10)–N(11)–N(12)	160(3)	N(3)–Co(1)–O(2)	93.60(14)
Fe–N(4)–N(5)	132.8(6)	N(4)–Co(2)–O(1)	95.84(14)
Fe–N(7)–N(8)	136.7(16)	N(4)–Co(2)–O(2)	93.18(13)
Fe–N(10)–N(11)	131.7(12)	N(5)–Co(2)–O(1)	1701.08(14)
		N(5)–Co(2)–O(2)	90.99(14)
		N(5)–Co(2)–O(4)	88.79(15)
		N(6)–Co(2)–O(1)	92.79(14)
		N(6)–Co(2)–O(2)	172.32(14)
		N(6)–Co(2)–O(4)	86.14(15)
		N(1)–Co(1)–N(2)	94.71(16)
		N(2)–Co(1)–N(3)	85.13(17)
		N(1)–Co(1)–N(3)	90.54(16)
		N(4)–Co(2)–N(5)	84.88(16)
		N(5)–Co(2)–N(6)	96.10(16)
		N(4)–Co(2)–N(6)	90.39(16)

Crystal structure of $[(L^2)Fe(N_3)_3]$ (3). The crystal structure of **3** is shown in Fig. 1 and selected bond lengths and angles are summarized in Table 2. The ligand L^2 binds the Fe(III) ion facially and the co-ordination geometry around the Fe(III) ion is a distorted octahedron. Two different Fe–N$_{azide}$ bond distances are observed [≈ 1.977 and 2.040 Å]; one of the distances is slightly shorter than that reported for an azido iron(III) tris(3,5-dimethyl-1-pyrazolyl)borate complex.[4b]
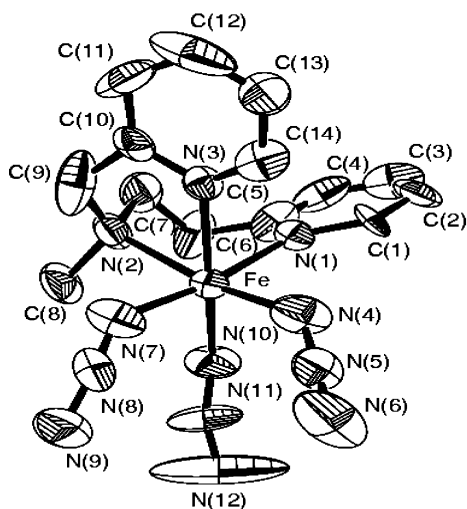
Fig. 1 Perspective view of the complex $[(L^2)Fe(N_3)_3]$, (**3**), showing the atom numbering. Atoms are drawn at the 50% probability level. Hydrogen atoms are omitted for clarity.

Crystal structure of $[(L^2)_2Fe_2(\mu\text{-}O)(\mu\text{-}O_2CMe)_2][ClO_4]_2\cdot 2H_2O$ (4). As already mentioned, due to the poor quality of the data set the refinement of the structure did not reach a satisfactory level. Nevertheless, the cation seems to have been determined well and a perspective view is shown in Fig. 2. The metrical parameters indicated the cation possesses well documented (μ-oxo)bis(μ-acetato)diiron(III) core.[4c,16–24] The L^2 ligand is co-ordinated to the metal centre in a facial mode as dictated by the orientation of the bridging ligands. The geometry at the iron atoms is approximately octahedral. Pertinent metric parameters: average Fe–O$_{oxo}$ bond length, Fe–O–Fe bond angle and Fe $\cdots$ Fe distance are 1.79 Å, 121.1° and 3.124 Å, respectively.
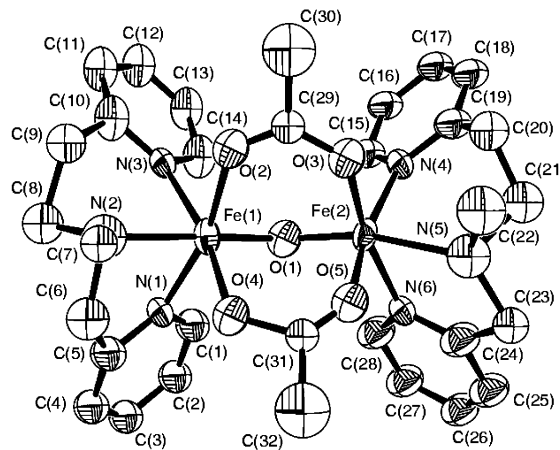
Fig. 2 View of the dication in crystals of $[(L^2)_2Fe_2(\mu\text{-}O)(\mu\text{-}O_2CMe)_2][ClO_4]_2\cdot 2H_2O$, (**4**), showing the atom numbering. Atoms are drawn at the 50% probability level. Hydrogen atoms are not included for clarity.

Crystal structure of $[(L^2)_2Co_2(\mu\text{-}OH)_2(\mu\text{-}O_2CMe)][ClO_4]_3\cdot MeCN$ (6). Fig. 3 shows the structure of a triply bridging tri-cation of complex **6**. It reveals that each of the two cobalt centres is in a pseudo-octahedral environment of a facially capping tridentate ligand L^2, two bridging OH groups, and an acetato bridge. While the pyridine ring with five-membered chelate rings is co-ordinated in a *cis* fashion to both the hydroxo groups, the pyridine ring with six-membered chelate ring is co-ordinated *cis* to one hydroxo group and *trans* to the other. The aliphatic nitrogen atoms are *trans* to the hydroxo groups. The two triply bridging dicobalt(III) unit is symmetrical (Table 2). While the average Co^{III}–O(hydroxo) bond distance is comparable to that reported by Wieghardt *et al.* for a triply-bridged mixed-valent complex with $\{Co^{III}Co^{II}(\mu\text{-}hydroxo)bis(\mu\text{-}acetato)\}^{2+}$ core; the average Co^{III}–O(acetate) distance is, however, slightly shorter in complex **6**, than the reported complex.[25]

Although several binuclear di-μ-hydroxo-bis[triammine-cobalt(III)] complexes with a carboxylato-bridging group are
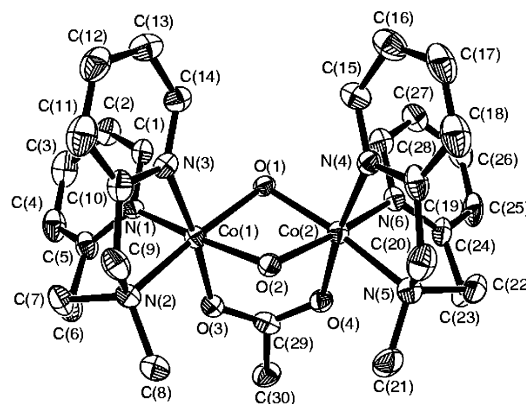
Fig. 3 View of the structure of the cation in crystals of $[(L^2)_2Co_2(\mu\text{-}OH)_2(\mu\text{-}O_2CMe)][ClO_4]_3\cdot MeCN$, (**6**), showing the atom numbering. Atoms are drawn at the 50% probability level. Hydrogen atoms are not included for clarity.

known in the literature,[26] to our knowledge, this is the first report of a dicobalt(III) complex with such a core with tridentate facially capping nonmacrocyclic ligand.

Magnetism

Monomeric complexes. The effective magnetic moment (μ_{eff}) values at 300 K for complexes **1**, **2** and **3** are 5.92, 5.83 and 5.86 μ_B, respectively. This clearly indicates high-spin d^5 electronic configuration of the iron(III) centres in monomeric complexes. From magnetic susceptibility measurements in the range 81–300 K, the Curie–Weiss plots [$\chi_M = C/(T - \theta)$] represent perfect $S = 5/2$ system (Fig. S1).† Solution-state (MeCN) data (5.87, 5.75 and 5.78 μ_B, respectively) justifies that the solid-state structures are retained in solution.

Dimeric complexes. As gross structural parameters are now available for **4** and **5**, for a meaningful comparative study, we performed magnetic susceptibility measurements of powdered samples of **4** and **5** in the temperature range 51–300 K by the Faraday method. It should be mentioned here that we[3] and others[5] reported temperature-dependent magnetic susceptibility measurements on **4** and green [(L^3)$_2$Fe$_2$(μ-O)(μ-O$_2$CMe)$_2$]-[ClO$_4$]$_2$·2H$_2$O (**5**) (*vide supra*), respectively. As reported previously[3,5] both complexes exhibit stong antiferromagnetic exchange coupling between the two Fe(III) centres. In fact, the values of effective magnetic moment (μ_{eff}/Fe) at 300 K/51 K are 1.62/0.30 μ_B for **4** and 1.74/0.38 μ_B for **5**. The results are shown in Fig. S2† in the form of $\chi_m T$ *vs.* T plots. The experimentally observed χ_m values (per dimer) may be expressed using the modified[3,13] expression (1),

$$\chi_m = \frac{Ng^2\beta^2}{kT} \frac{[2e^{2x} + 10e^{6x} + 28e^{12x} + 60e^{20x} + 110e^{30x}]}{[1 + 3e^{2x} + 5e^{6x} + 7e^{12x} + 9e^{20x} + 11e^{30x}]}(1 - \rho)$$
$$+ (Ng^2\beta^2/3kT)S(S + 1)\rho \qquad (1)$$

where $x = J/kT$, N, g and k have their usual meanings and ρ is the mole fraction of the non-coupled iron(III) imputity. The singlet–triplet energy gap is expressed in terms of 2J. The J and ρ parameters were determined by minimizing

$$R = \sum (\chi_m{}^{obs} - \chi_m{}^{calc})^2 \Big/ \sum (\chi_m{}^{obs})^2.$$

Non-linear regression analysis (g was fixed at 2.00) of the data using eqn. (1) gave good data fits: $J = -130$ cm^{-1}, $\rho = 0.0047$ and $R = 2.19 \times 10^{-8}$ for **4**; $J = -114$ cm^{-1}, $\rho = 0.0069$ and $R = 7.78 \times 10^{-9}$ for **5**. Thus we can infer that for two diiron(III) complexes containing the (μ-oxo)bis(μ-acetato)diiron(III) core capped by two closely similar tridentate facially capping ligands, the complex with unsymmetrical ligand gives rise to enhanced antiferromagnetic exchange coupling between the two Fe(III) centres.

In MeCN, the effective magnetic moment per iron atom (μ_{eff}/Fe) values determined by Evans method are 1.70 for **4** and 1.73 for **5**, respectively. These data are in reasonable agreement with that obtained in the solid-state (*vide supra*). The dicobalt(III) complex **6** is diamagnetic, as expected.

Magneto-structural trend. A critical analysis of X-ray structures of complexes containing a (μ-oxo)bis(μ-carboxylato)-diiron(III) core capped by tridentate facially capping N-donor ligands reveal the following structural parameter ranges: average Fe–O(oxo) distance, 1.78–1.80 Å; average Fe–O–Fe angles, 117–126°; average Fe $\cdots$ Fe distances, 3.06–3.17 Å.[4c,16–24] Among this class of structurally characterized complexes for which magnetic studies have been carried out (one complex has a dimer-of-dimers type structure),[23] the $-J$ values representing antiferromagnetic exchange coupling (the singlet–triplet energy gap is expressed in terms of 2J values), all occur in the range 84–134 cm^{-1}.[2b,16–24]

Based on the observed results Fenton and co-workers attempted[19] to arrive at a magneto-structural trend. It was realized that greater the Fe $\cdots$ Fe distance the stronger is the magnitude of the antiferromagnetic exchange coupling. This relationship is mediated by the Fe–O(oxo)–Fe angle; greater coupling being a result of a more obtuse arrangement,[27] the consequence of which is a longer Fe $\cdots$ Fe distance. For **4** and **5** the J values obtained from this investigation are in good agreement with their prediction. It should be noted that for **4/5** average Fe–O$_{oxo}$ bond length, Fe–O–Fe bond angle and Fe $\cdots$ Fe distance are: Fe–O$_{oxo}$ bond length 1.79/1.788 Å, Fe(1)–O(1)–Fe(2) angle 121.1°/118.2° and the non-bonding Fe $\cdots$ Fe distance is 3.124/3.068 Å, respectively.

Notably, a detailed theoretical analysis by using an angular and radial overlap model revealed[28] that the magnetic properties of these complexes depend on the iron–(μ-O) distance as well as on the iron–(μ-O)–iron angle. Considering a group of dibridged (μ-oxo)diiron(III) complexes Que *et al.*[29] claimed that the Fe–O–Fe angle has little effect on the magnitude of the coupling between the iron centres. According to the quantitative magneto-structural relationship by Gorun and Lippard,[30] the J values for **4** and **5** are predicted to be -119 cm^{-1} and -129 cm^{-1}, respectively. These values not only do not conform to that observed in this study but the trend is also reversed. We are not in a position to make a comment on this observation.

Spectral properties

The electronic spectra of **1**, **2** and **3** in MeCN show ligand-to-metal charge-transfer bands: 309 and 356 nm [Cl$^-$ $\longrightarrow$ Fe(III)] for **1**; 304 and 372 nm [Cl$^-$ $\longrightarrow$ Fe(III)] for **2** and 332 and 506 nm [N$_3^-$ $\longrightarrow$ Fe(III)] for **3**. Intraligand transitions are observed at still higher energies. Fig. 4 displays the behaviour of **2** and **3**. The electronic spectral feature of **4** in MeCN solution was reported earlier.[3] In MeCN solution **5** exhibits an identical electronic spectrum to that reported for the green form of this complex (Fig. S3).[5] Fig. 4 also shows the absorption spectrum of
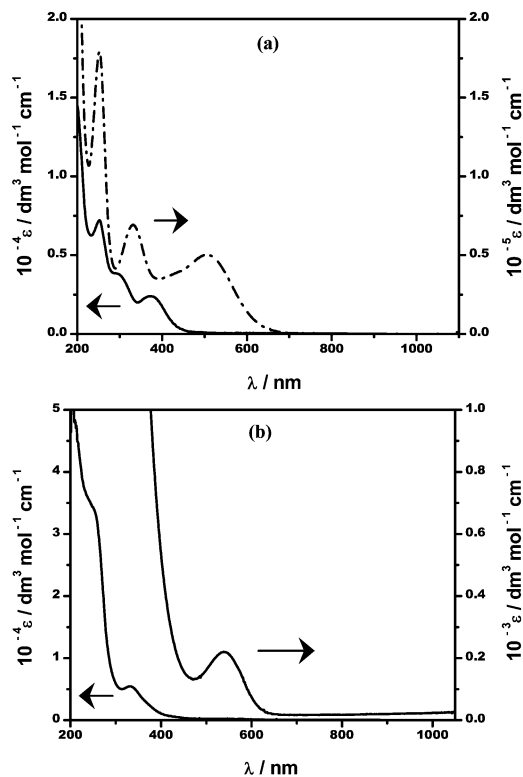
Fig. 4 Electronic spectra of (a) [(L^3)FeCl$_3$]·H$_2$O, (**2**), (solid line) and [(L^2)Fe(N$_3$)$_3$], (**3**), (broken line) and (b) [(L^2)$_2$Co$_2$(μ-OH)$_2$(μ-O$_2$CMe)] [ClO$_4$]$_3$·MeCN, (**6**), in MeCN.

$[(L^2)_2Co_2(\mu\text{-}OH)_2(\mu\text{-}O_2CMe)][ClO_4]_3\cdot CH_3CN$ (**6**), which is very similar to those reported for related species with $\{Co^{III}_2\text{-}(\mu\text{-}OH)_2(\mu\text{-}O_2CMe)\}^{3+}$ core. It consists of only one d–d band at 540 nm ($^1A_{1g} \rightarrow {}^1T_{1g}$ in O_h symmetry); the intense absorption at 330 nm must be due to $OH^- \rightarrow Co(III)$ charge-transfer transition.[25,26a]

Redox properties

The purpose of cyclic voltammetric (CV) measurements was to determine whether or not between the complexes **1** and **2**, and **4** and **5**, the effect of ligand chelate-ring size on the Fe^{III}/Fe^{II} redox potential (V *vs.* SCE) could be identified. A comparative study between **1** and **3** is expected to reveal the relative strength of anionic ligands Cl^-/N_3^- to stabilize the Fe(III) state towards reduction. The CV scans of **1** and **2** in MeCN at a glassy-carbon working electrode reveal a well-formed cathodic peak [E_{pc} (cathodic peak potential) = -0.04 for **1** and -0.06 for **2**] and during the anodic (re-oxidation) scan two responses were observed: 0.04 V and 0.40 V for **1** and 0.04 and 0.38 for **2**. This behaviour is typical of electron transfer followed by chemical reaction. In fact, the nature of the CV of **1** and **2** implies partial Cl^- dissociation after reduction of the Fe(III) centre, which is exemplified by the observation of two responses during the anodic scan. The azido complex **3**, however, displays (Fig. 5) a quasi-reversible Fe^{III}/Fe^{II} redox process ($E_{1/2} = -0.22$ V and $\Delta E_p = 160$ mV).[8] Hence, N_3^- is a better stabilizer of Fe(III) state than Cl^- towards reduction.

The CV scans of **4** and **5** at a platinum working electrode are shown in Fig. 5. During the cathodic scan of **4**, a reduction wave is seen at -0.40 V for which there appears to be no corresponding oxidation wave (two small inflections can be seen at 0.26 and 0.40 V), indicating that the $Fe^{III}Fe^{III} \rightarrow Fe^{III}Fe^{II}$ reduction process is completely irreversible. A similar instability with respect to electrochemical reduction was observed in $[Fe_2O(O_2CMe)_2\{HB(pz)_3\}_2]$, for which an irreversible reduction occurred at -0.76 V *vs.* SCE.[17b] The CV behaviour of **5** differs considerably from that of **4**, exhibiting a quasi-reversible $Fe^{III}Fe^{III} \rightarrow Fe^{III}Fe^{II}$ redox process: $E_{1/2} = -0.32$ V and $\Delta E_p = 200$ mV. Here also a small inflection can be seen at 0.20 V on the anodic scan. It is worth mentioning here that Hartman *et al.* observed a quasi-reversible wave at -0.37 V *vs.* SCE for $[Fe_2O(O_2CMe)_2(Me_3TACN)_2][PF_6]_2$.[17d] The observation of E_{pc} for **4** at a less negative potential indicates that the $Fe^{III}Fe^{II}$ species generated on the CV time-scale is less stable in the case of L^3 than that with L^2. We attribute the shift in E_{pc} values to the increased electron donating effect of L^3, due to the formation of two five-membered chelate rings in L^3, than that of a five-membered and a six-membered chelate ring in L^2. In essence, the $Fe^{III}Fe^{III}$ state is better stabilized by L^3 than L^2, with respect to reduction to the $Fe^{III}Fe^{II}$ state.

The triply-bridged dicobalt(III) complex **6** displays in MeCN a quasi-reversible reductive response ($E_{1/2} = 0.22$ V and $\Delta E_p = 200$ mV) corresponding to the $Co^{III}Co^{III}$ to $Co^{III}Co^{II}$ state (Fig. 5). Given the larger ΔE_p value of this redox process it is understandable that the mixed-valence form is not expected to be stable, at least on the CV time scale.

Conclusion

Synthesis of $[(L^2/L^3)Fe^{III}Cl_3]\cdot H_2O$ and successful preparation and structural characterization of $[(L^2)Fe^{III}(N_3)_3]$ illustrates that $[(L^2/L^3)FeCl_3]\cdot H_2O$ can be useful starting materials for the synthesis of interesting iron complexes.[4c] The X-ray structural results on triply-bridged diiron(III) complex **4** presented here underpin the significance of the magneto-chemical properties observed before.[3] Comparative magnetic studies between complexes **4** and **5** with $\{Fe^{III}_2(\mu\text{-}O)(\mu\text{-}O_2CMe)_2\}^{2+}$ core, point to the existence of enhanced antiferromagnetic exchange couplings in **4**. This result reveals the significance of the
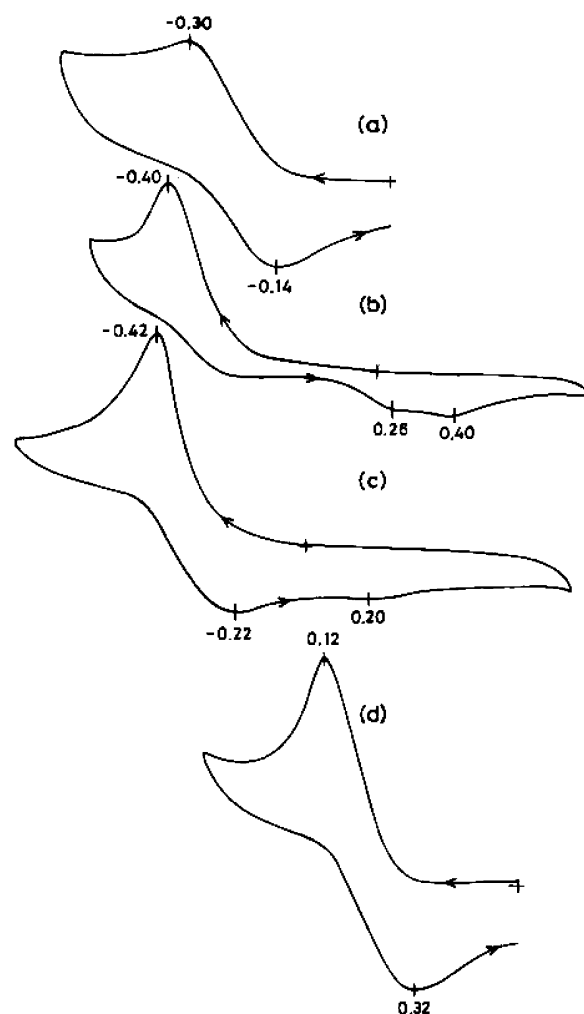
Fig. 5 Cyclic voltammograms of (a) $[(L^2)Fe(N_3)_3]$, (**3**), (b) $[(L^2)_2Fe_2(\mu\text{-}O)(\mu\text{-}O_2CMe)_2][ClO_4]_2\cdot 2H_2O$, (**4**), (c) $[(L^3)_2Fe_2(\mu\text{-}O)(\mu\text{-}O_2CMe)_2][ClO_4]_2\cdot 2H_2O$, (**5**), and (d) $[(L^2)_2Co_2(\mu\text{-}OH)_2(\mu\text{-}O_2CMe)][ClO_4]_3\cdot MeCN$, (**6**), in MeCN. Experimental conditions: supporting electrolyte, 0.1 mol dm^{-3} [NBu$^n_4$][ClO$_4$]; working electrode: glassy-carbon (complexes **1–3**) and platinum (complexes **4–6**); [complex] $\approx 10^{-3}$ mol dm^{-3}; temperature 25 °C.

unsymmetrical ligand in providing a better magnetic exchange pathway (enhanced Fe–Fe distance) than that with a symmetrical ligand. Our goal of synthesising a dicobalt(III) complex containing the triply-bridged core $\{Co^{III}_2(\mu\text{-}OH)_2(\mu\text{-}O_2CMe)\}^{3+}$ has been achieved by using L^2 as a terminal facially capping ligand. To the best of our knowledge, this is the only structural report of such a core formation with facially capping tridentate N-donor ligands, used in syntheses of triply-bridged dimetal centres.

References

1 (*a*) P. C. Wilkins and R. G. Wilkins, *Coord. Chem. Rev.*, 1987, **79**, 195; (*b*) R. E. Stenkamp, *Chem. Rev.*, 1994, **94**, 715; (*c*) J. Du Bois, T. J. Mizoguchi and S. J. Lippard, *Coord. Chem. Rev.*, 2000, **200–202**, 443 and references therein.

2 (*a*) L. Que, Jr. and A. E. True, *Prog. Inorg. Chem.*, 1990, **38**, 97; (*b*) D. M. Kurtz, Jr., *Chem. Rev.*, 1990, **90**, 585; (*c*) J. B. Vincent, G. L. Olivier-Lilley and B. A. Averill, *Chem. Rev.*, 1990, **90**, 1447.

3 S. Mahapatra, N. Gupta and R. Mukherjee, *J. Chem. Soc., Trans.*, 1992, 3041.

4 (*a*) K. Wieghardt, K. Pohl and D. Ventur, *Angew. Chem., Int. Ed. Engl.*, 1985, **24**, 392; (*b*) H. Fukui, M. Ito, Y. Moro-oka and N. Kitajima, *Inorg. Chem.*, 1990, **29**, 2868; (*c*) S.-H. Cho, D. Whang, K.-N. Han and K. Kim, *Inorg. Chem.*, 1992, **31**, 519; (*d*) G. C. Silver and W. C. Trogler, *J. Am. Chem. Soc.*, 1995, **117**, 3983; (*e*) R. Lescouëzec, J. Vaissermann, F. Lloret, M. Julve and M. Verdaguer, *Inorg. Chem.*, 2002, **41**, 5943.

5 K. B. Jensen, C. J. McKenzie, O. Simonsen, H. Toftlund and A. Hazell, *Inorg. Chim. Acta*, 1997, **257**, 163.

6 (*a*) T. K. Lal and R. Mukherjee, *Inorg. Chem.*, 1998, **37**, 2373; (*b*) V. Balamurugan, R. Gupta, P. K. Chowdhury and R. Mukherjee, manuscript in preparation.

7 (*a*) S. Mahapatra, P. Das and R. Mukherjee, *J. Chem. Soc., Dalton Trans.*, 1993, 217; (*b*) S. Mahapatra, T. K. Lal and R. Mukherjee, *Inorg. Chem.*, 1994, **33**, 1579.

8 N. Gupta, S. Mukherjee, S. Mahapatra, M. Ray and R. Mukherjee, *Inorg. Chem.*, 1992, **31**, 139 and references therein.

9 W. H. Armstrong and S. J. Lippard, *Inorg. Chem.*, 1985, **24**, 981.

10 W. J. Geary, *Coord. Chem. Rev.*, 1971, **7**, 81.

11 R. Gupta, S. Mukherjee and R. Mukherjee, *J. Chem. Soc., Dalton Trans.*, 1999, 4025 and references therein.

12 D. F. Evans, *J. Chem. Soc.*, 1959, 2003.

13 C. J. O'Connor, *Prog. Inorg. Chem.*, 1982, **29**, 203.

14 L. J. Farrugia, WINGX ver 1.64 (2003), An Integrated Systems of Windows programs for the Solution, Refinement, and Analysis of single crystal X-ray diffraction data, Department of Chemistry, University of Glasgow.

15 J. L. Sessler, J. W. Sibert and V. Lynch, *Inorg. Chem.*, 1990, **29**, 4143.

16 (*a*) K. Wieghardt, K. Pohl and W. Gebert, *Angew. Chem., Int. Ed. Engl.*, 1983, **22**, 727; (*b*) K. Wieghardt, K. Pohl and D. Ventur, *Angew. Chem., Int. Ed. Engl.*, 1985, **24**, 392; (*c*) P. Chaudhuri, K. Wieghardt, B. Nuber and J. Weiss, *Angew. Chem., Int. Ed. Engl.*, 1985, **24**, 778.

17 (*a*) W. H. Armstrong and S. J. Lippard, *J. Am. Chem. Soc.*, 1983, **105**, 4837; (*b*) W. H. Armstrong, A. Spool, G. C. Papaefthymiou, R. B. Frankel and S. J. Lippard, *J. Am. Chem. Soc.*, 1984, **106**, 3653; (*c*) A. Spool, I. D. Williams and S. J. Lippard, *Inorg. Chem.*, 1985, **24**, 2156; (*d*) J. R. Hartman, R. L. Rardin, P. Chaudhuri, K. Pohl, K. Wieghardt, B. Nuber, J. Weiss, G. C. Papaefthymiou, R. B. Frankel and S. J. Lippard, *J. Am. Chem. Soc.*, 1987, **109**, 7387.

18 P. Gomez-Romero, N. Casan-Pastor, A. Ben-Hussein and G. B. Jameson, *J. Am. Chem. Soc.*, 1988, **110**, 1988.

19 H. Adams, N. A. Bailey, J. D. Crane, D. E. Fenton, J.-M. Latour and J. M. Williams, *J. Chem. Soc., Dalton Trans.*, 1990, 1727.

20 F.-J. Wu, D. M. Kurtz, Jr., K. S. Hagen, P. D. Nyman, P. G. Debrunner and V. A. Vankai, *Inorg. Chem.*, 1990, **29**, 5174.

21 M. Kodera, H. Shimakoshi, M. Nishimura, H. Okawa, S. Iijima and K. Kano, *Inorg. Chem.*, 1996, **35**, 4967.

22 H. Toftlund, K. S. Murray, P. R. Zwack, L. F. Taylor and O. P. Anderson, *J. Chem. Soc., Chem. Commun.*, 1986, 191.

23 N. Arulsamy, J. Glerup and D. J. Hodgson, *Inorg. Chem.*, 1994, **33**, 3043.

24 K. J. Oberhausen, J. F. Richardson, R. J. O'Brien, R. M. Buchanan, J. K. McCusker, R. J. Webb and D. N. Hendrickson, *Inorg. Chem.*, 1992, **31**, 1123.

25 P. Chaudhuri, J. Querbach, K. Wieghardt, B. Nuber and J. Weiss, *J. Chem. Soc., Dalton Trans.*, 1990, 271.

26 (*a*) K. Wieghardt, *J. Chem. Soc., Dalton Trans.*, 1973, 2548; (*b*) K. Wieghardt, W. Schmidt, B. Nuber and J. Weiss, *Chem. Ber.*, 1979, **112**, 2220.

27 R. Mukherjee, T. D. P. Stack and R. H. Holm, *J. Am. Chem. Soc.*, 1988, **110**, 1850.

28 H. Weihe and H. U. Güdel, *J. Am. Chem. Soc.*, 1997, **119**, 6539.

29 R. E. Norman, R. C. Holz, S. Ménage, C. J. O'Connor, J. H. Zhang and L. Que, Jr., *Inorg. Chem.*, 1990, **29**, 4629.

30 S. M. Gorun and S. J. Lippard, *Inorg. Chem.*, 1991, **30**, 1625.